Ca^{2+}-activated myosin-ATPases, creatine and adenylate kinases regulate mitochondrial function according to myofibre type in rabbit

N. Gueguen, L. Lefaucheur, P. Ecolan, M. Fillaut and P. Herpin

INRA, Unité Mixte de Recherche Système d'Elevage Nutrition Animale et Humaine, Domaine de la Prise, 35590 Saint-Gilles, France

Mitochondrial respiration rates and their regulation by ADP, AMP and creatine, were studied at different free Ca^{2+} concentrations (0.1 *versus* 0.4 μM) on permeabilized fibre bundles of rabbit skeletal muscles differing in their myosin heavy chain profiles. Four fibre bundle types were obtained: pure types I and IIx, and mixed types IIax (approximately 50% IIa and 50% IIx fibres) and IIb+ (60% IIb fibres, plus IIx and IIa). At rest, pure type I fibres displayed a much higher apparent K_m for ADP (212 μM) than IIx fibres (8 μM). Within the IIax and IIb+ mixed fibre bundle types, two K_m^{ADP} values were observed (70 μM and 5 μM). Comparison between pure IIx and mixed types indicates that the intermediate K_m of 70 μM most probably corresponds to the mitochondrial affinity for ADP in IIa fibres, the lowest K_m for ADP (5 μM) corresponding to IIx and IIb types. Activation of mitochondrial creatine and adenylate kinase reactions stimulated mitochondrial respiration only in type I and IIax fibre bundles, indicating an efficient coupling between both kinases and ADP rephosphorylation in type I and, likely, IIa fibres, since no effect was observed in pure IIx fibres. Following Ca^{2+}-induced activation of myosin-ATPase, an increase in mitochondrial sensitivity to ADP of 45% and 250% was observed in type IIax and I bundles, respectively, an effect mostly prevented by addition of vanadate, an inhibitor of myosin-ATPase. Ca^{2+}-induced activation of myosin-ATPase also prevented the stimulation of respiration rates by creatine and AMP in I and IIax bundles. In addition to differential regulation of mitochondrial respiration and energy transfer systems at rest in I and IIa *versus* IIx and IIb muscle fibres, our results indicate a regulation of phosphotransfer systems by Ca^{2+} via the stimulation of myosin-ATPases in type I and IIa fibres of rabbit muscles.

(Resubmitted 11 January 2005; accepted after revision 18 February 2005; first published online 24 February 2005)
Corresponding author L. Lefaucheur: INRA, Unité Mixte de Recherche SENAH, Domaine de la Prise, 35590 Saint-Gilles, France. Email: louis.lefaucheur@rennes.inra.fr

Understanding the mechanisms of regulation of mitochondrial function and energy transfer between spatially separated intracellular ATP production and consumption is an important issue of muscle bioenergetics. Skeletal muscle is a heterogeneous tissue mostly composed of functionally diverse fibre types. Four contractile fibre types have been identified in adult mammalian skeletal muscles, i.e. types IIb, IIx, IIa and I; they exhibit decreasing maximal shortening velocities in this rank order (Pellegrino *et al.* 2003). The relative importance of the two metabolic pathways of energy production, i.e. glycolysis and mitochondrial oxidative phosphorylation, varies between muscle types depending on their contractile patterns. The fast type IIx and IIb fibres are adapted to brief and intense contractions fuelled by the glycolytic pathway and immediate availability of phosphocreatine; the slow type I fibres can sustain prolonged low power work in association with a well-developed oxidative metabolism. Type IIa fibres are oxido-glycolytic and exhibit intermediate contractile function. Because of the differential energy demands and dependence on mitochondria between fibre types, specific tuning of mitochondrial function and specialized energy transfer pathways can be expected in the different contractile fibre types to match ATP synthesis with its utilization. Indeed, slow-twitch muscle fibres display a much higher apparent K_m of oxidative phosphorylation for ADP (K_m^{ADP}) than fast-twitch fibres (Veksler *et al.* 1995; Kuznetsov *et al.* 1996; Kay *et al.* 1997; Burelle & Hochachka, 2002; Zoll *et al.* 2002), which is likely to be due to a low permeability of the outer mitochondrial membrane (OMM) to ADP in the former (Saks *et al.* 1993; Kay *et al.* 1997; Appeix *et al.* 2003). Thus, differential regulation of mitochondrial respiration clearly occurs

 DOI: 10.1113/jphysiol.2005.083030

among slow and fast muscle types, but whether respiration regulation also differs within subtype II fibres is not documented.

Fibre types also differ according to the control of respiration by mitochondrial kinases. Indeed, creatine has been shown to increase ADP-stimulated respiration in slow-twitch muscles, due to a functional coupling between mitochondrial creatine kinase (mtCK), adenine nucleotide translocase (ANT) and porin (voltage-dependent anion channel, VDAC) (Wallimann *et al.* 1992; Saks *et al.* 1994; Kay *et al.* 2000). Such a coupling does not occur in fast-twitch muscles (Veksler *et al.* 1995; Kay *et al.* 2000). Considering this functional coupling and the restricted permeability of OMM for ADP, mtCK appears to be a good candidate to control the metabolic fluxes between mitochondria and cytoplasm in slow-twitch muscle. Therefore, mtCK, together with the cytosolic isoform of CK (MM-CK), located in close proximity to the myofibrils, has been proposed to be involved in energetic communication by efficiently transferring energy-rich phosphoryls from mitochondria to myofibrillar Ca-ATPase (Wallimann *et al.* 1992; Saks *et al.* 1994; Kay *et al.* 2000; Joubert *et al.* 2002). However, muscle performance and metabolic integrity were altered less than expected when CK activity was markedly suppressed or deleted (Veksler *et al.* 1995; Steeghs *et al.* 1997; Saupe *et al.* 1998; Bruton *et al.* 2003), suggesting that alternative phosphotransfer pathways are also involved. A candidate enzyme is adenylate kinase (AK). Indeed, two main AK isoenzymes, basic (AK1, cytosolic) and acidic (AK2, mitochondrial), have been reported in many tissues including heart and skeletal muscle fibres (Watanabe *et al.* 1979; Walker & Dow, 1982; Hamada *et al.* 1987). Moreover, a functional coupling between AK1 and myofibrillar ATPase has been demonstrated by Savabi *et al.* (1986). In the heart, AK2 has been involved in the control of oxidative phosphorylation (Dzeja *et al.* 1983; Clark *et al.* 1997) and export and transfer (Dzeja *et al.* 1985, 1999) of high-energy phosphoryls from mitochondria to actomyosin. To our knowledge, the functional coupling between AK2 and mitochondrial oxidative phosphorylation has not been investigated in skeletal muscle fibres.

Calcium ions are major regulatory and signalling agents in all muscle fibres. Besides the well-known Ca^{2+}-triggered fibre contraction linked to the activation of actomyosin-ATPase through the troponin system, Ca^{2+} may also be involved in the adaptation of mitochondrial function to the dramatic increase of energy demand in contracting fibres (Berchtold *et al.* 2000; Martonosi & Pikula, 2003). Thus, Ca^{2+} and/or contractile activity may be involved in regulation of mitochondrial respiration and energy transfer. Indeed, it has been suggested that the contribution of the AK and CK enzyme systems to the overall energy transfer relies on muscle fibre activity (Zeleznikar *et al.* 1990; Dzeja *et al.* 1996, 1999; Joubert *et al.* 2002). However, most of the studies on permeabilized fibres are performed in resting conditions, i.e. pCa = 7, and further work is needed to address the regulatory effect of Ca^{2+} on energy production and transfer among the different contractile fibre types.

Therefore, the present experiment was undertaken in an attempt to determine the influence of fibre contractile type and Ca^{2+}-induced myosin-ATPase activation on the functional coupling between mitochondrial kinases and oxidative phosphorylation and on mitochondrial ADP sensitivity. For this purpose, mitochondrial respiration rates and their regulation by ADP, creatine and AMP at different free Ca^{2+} concentrations, and in the absence or presence of the myosin inhibitor, vanadate, were measured *in situ* on permeabilized fibres differing in their myosin heavy chain (MyHC) profiles.

Methods

Animals and tissue sampling

The experiments reported herein complied with French national regulations for the care and use of animals in research and were approved by the local Animal Care Committee (the local Authority of Veterinary Services). The study was conducted on 26 male New Zealand White rabbits, housed individually in cages placed in a thermoneutral environment ($20 \pm 1^{\circ}$C) and fed standard commercial diet and water *ad libitum*. Animals were killed at the age of 11 weeks (2.3–2.5 kg body weight) by electrical stunning and exsanguination. Immediately after killing, four muscles were excised and placed in precooled relaxing solution A containing (mM): CaK_2EGTA 2.77, K_2EGTA 7.23, $MgCl_2$ 6.56, DTT 0.5, potassium 2-(*N*-morpholino)ethansulphonate (K-Mes) 50, imidazole 20, taurine 20, ATP 5.3, phosphocreatine 15, pH 7.1 adjusted at 4°C (free Ca^{2+} concentration 0.1 μM, a condition which prevents contraction of the bundles) (Saks *et al.* 1998). The semimembranosus proprius (SmP), tibialis anterior (TA), psoas major (PM), and semimembranosus accessoris (SmA) muscles were selected based on their contractile properties, i.e. type I, IIa plus IIx, IIx, and mostly IIb, respectively (Gondret *et al.* 1996; McKoy *et al.* 1998).

Preparation of saponin-permeabilized muscle fibres

Saponin-permeabilized fibres were prepared from the four muscles as previously described (Saks *et al.* 1998). Briefly, thin fibre bundles (5–8 mm long, about 1 mm wide) were excised along the fibre orientation to avoid mechanical damage of the cells. Fibres were carefully separated from each other using sharp-ended forceps and needles in cooled solution A until bundles of roughly 20–30 fibres

were obtained with only small areas of contact between them. Fibres were then permeabilized by incubation in solution A supplemented with 50 μg ml^{-1} saponin with gentle shaking for 30 min at 4°C. To completely remove all metabolites, including trace amounts of ADP, fibres were washed three times in respiration solution B (mM: CaK_2EGTA 2.77, K_2EGTA 7.23, $MgCl_2$ 1.38, DTT 0.5, K-Mes 100, imidazole 20, taurine 20, and K_2HPO_4 3, pH 7.1 adjusted at 25°C, free Ca^{2+} concentration 0.1 μM) supplemented with bovine serum albumin (2 mg ml^{-1}). Before respiration measurements, a 1-mm-thick transverse section of each fibre bundle was immersed in 100 μl of 1 × Laemmli solution (Sigma, S-3401), boiled for 4 min at 100°C and stored at −80°C for further MyHC content analysis. The remaining bundle portions were kept on ice in solution B for high-resolution respirometry analysis.

High-resolution respirometry

Respiratory parameters of fibre bundles (20–30 fibres) were recorded at 25°C using a two-channel high-resolution respirometer (Oroboros oxygraph-2 k, Oroboros, Innsbruck, Austria), in 2-ml glass chambers containing solution B supplemented with bovine serum albumin (2 mg ml^{-1}). The medium was equilibrated for 30 min in air in the oxygraph chambers and stirred at 700 r.p.m. until a stable signal was obtained for calibration at air saturation. The corresponding oxygen concentration was calculated from the digitally recorded barometric pressure and the oxygen solubility at 25°C (Oroboros Bioenergetic News 6.3, http//www.oroboros.at) and digitally corrected for background flux, measured in separate controls using the same medium without biological material (Gnaiger, 2001).

Quality control

The quality of the permeabilized fibre preparations was assessed each day of the respiration experiments, and all met the quality criteria defined by Saks *et al.* (1998): (i) full permeabilization was checked by the absence of any increase in the maximal ADP-stimulated respiration rate following addition of the uncoupler, carbonyl cyanide 4-(trifluoromethoxy)phenylhydrazone (FCCP); (ii) complete removal of ADP could be easily shown by low and reproducible resting respiration rates not sensitive to ANT inhibition by atractyloside; (iii) addition of exogenous cytochrome *c* (Cyt *c*) did not further increase the maximal ADP-stimulated respiration rate, which strongly supports OMM intactness; (iv) finally, the quality of our preparations was confirmed by the linearity of the respiration rates with saturating concentration of ADP (1 mM) for at least 15 min of respiration recording. Four types of analyses (see below) were conducted on the four muscles studied. For technical reasons, these four analyses were conducted on different animals to allow measurements on the four muscles from the same rabbit each day. The experiments were repeated six to eight times giving a total of 26 animals.

Respiration rates and acceptor control ratio (ACR)

Resting respiration (V_0) was initiated in the presence of complex I substrates, 5 mM malate and 5 mM pyruvate, and maximal ADP-stimulated respiration was measured with one addition of saturating ADP concentration (1 mM). The ACR, defined as V_{max}/V_0 where V_{max} is $V_{(ADP\ 1\ mM)} + V_0$, was used to evaluate the coupling of respiration to phosphorylation (Saks *et al.* 1998).

Regulation of respiration by ADP

Kinetics of respiration rates were determined, in the presence of malate and pyruvate, by stepwise increases of ADP concentration from 0.01 to 1 mM, followed by addition of 1 μM FCCP (maximal respiration). The ADP-stimulated respiration above V_0 was plotted as a function of ADP concentration, and the K_m^{ADP} was estimated using the linearization method of Lineweaver–Burk (Jacobus *et al.* 1982).

Coupling between mitochondrial kinases and oxidative phosphorylation

A titration protocol was developed to analyse the effects of the activation of some mitochondrial kinases (mtCK, AK2) and mitochondria-bound hexokinase (HK1) on ADP kinetic parameters (Fig. 1). In the first bundle from each muscle: (i) V_0 was initiated by the addition of 5 mM malate and 5 mM pyruvate; (ii) submaximal ADP-stimulated respiration was induced by 0.1 mM ADP; followed by (iii) the addition of 0.9 mM ADP (1 mM final concentration, maximal ADP-stimulated respiration); (iv) finally, Cyt *c* was added (8 μM) to check OMM intactness and uncoupled respiration was measured in the presence of 1 μM FCCP. In a second fibre bundle, the same titration protocol was used, except that 20 mM creatine (mtCK activation) was added after step (ii). Finally, in a third fibre bundle, 10 mM glucose (HK1 activation), 1 mM AMP (AK2 activation) and 10 μM Ap5A (AK2 inhibition; Valentine *et al.* 1989) were successively added between steps (ii) and (iii). The absence of interactions between glucose and AMP was checked during preliminary tests (data not shown).

Free Ca^{2+} effect on mitochondrial respiration regulation

The titration protocol was repeated but 5.5 mM $CaCl_2$ (0.4 μM free Ca^{2+} concentration) was added after step (ii). The total calcium concentration necessary to achieve 0.4 μM free Ca^{2+} was calculated using the WINMAXC

program (Standford University, CA, USA) with the following values: pH 7.1; temperature 25°C; ionic strength 175 mM; ADP 0.1 mM, EGTA 10 mM; Mg^{2+} 4 mM. This free Ca^{2+} concentration has been shown to be sufficient and optimal for Ca^{2+}-ATPase activation (Kummel, 1988). The measurements were performed in the absence or presence of 0.6 mM vanadate, an inhibitor of myosin-ATPases (Kunz *et al.* 1993). The absence of any effect of vanadate alone (without calcium) on mitochondrial respiration parameters (V_0, V_{max}, ADP and creatine sensitivity) was checked and confirmed during preliminary experiments. The sensitivity to ADP was estimated in all the experiments from the ratio between respiration rates at 0.1 and 1 mM ADP (ADP sensitivity index). This index gives a valuable estimation of ADP sensitivity when the titration protocol does not allow K_m^{ADP} measurement (Tonkonogi *et al.* 1998).

In all the experiments, the exact ADP concentration in stock solutions was determined spectrophotometrically at 259 nm. After each experiment, fibre bundles were

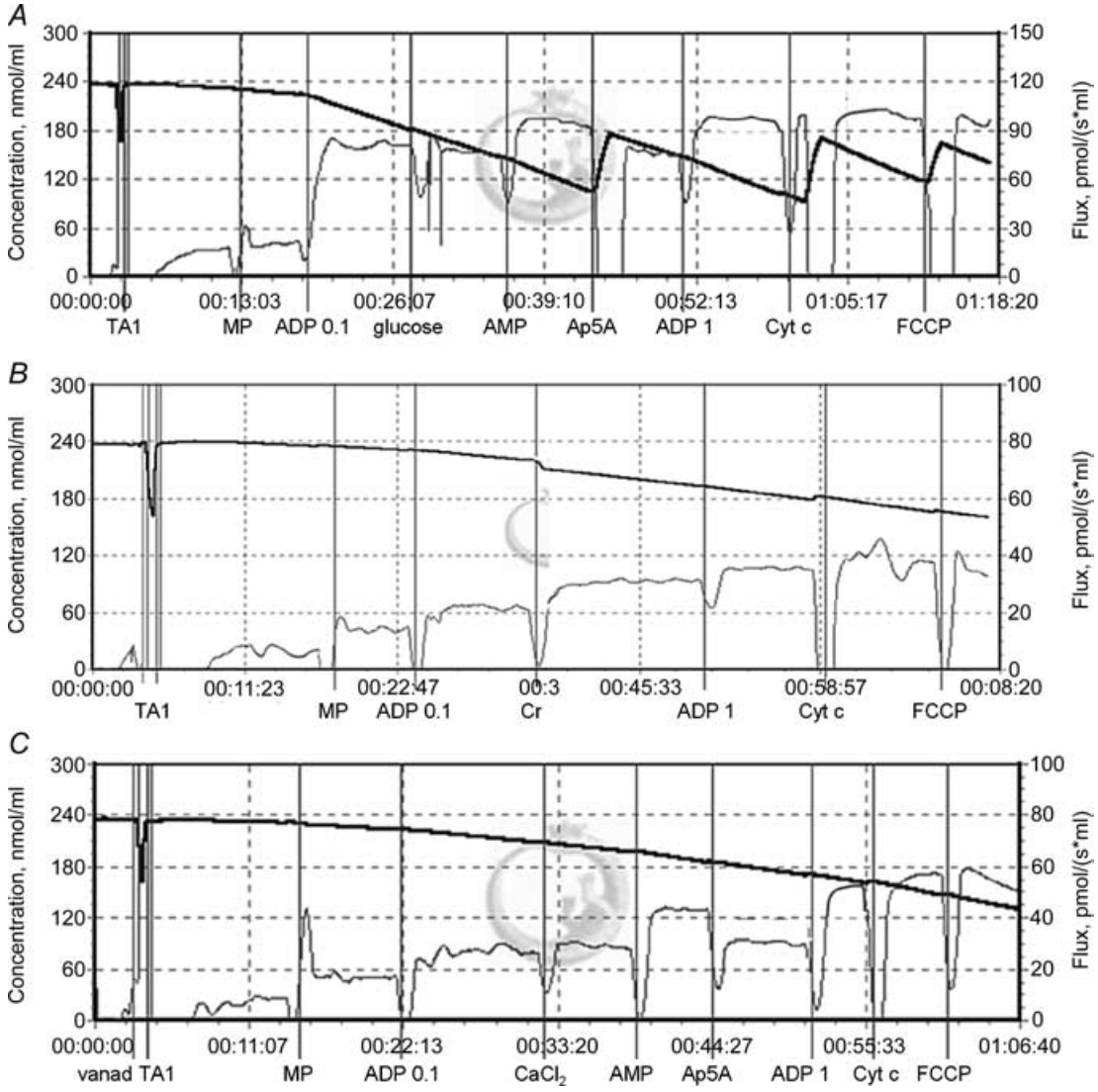

Figure 1. Titration protocols used to analyse the effect of mitochondrial and mitochondria-bound kinase activation on submaximal respiration rate

After the addition of fibre bundle (TA1) and malate plus pyruvate (MP), respiration was stimulated by 0.1 mM ADP. *A*, mitochondria-bound hexokinase HK1 and adenylate kinase AK2 were activated by 10 mM glucose and 1 mM AMP, respectively, and AK2 was then inhibited by 10 μM Ap5A. *B*, mitochondrial creatine kinase (mtCK) was activated by 20 mM creatine (Cr). *C*, effect of 0.4 μM free Ca^{2+} in the presence of 0.6 mM vanadate, followed by stimulation (AMP) and inhibition (Ap5A) of AK2. All protocols ended by successive additions of 1 mM ADP, 8 μM Cyt *c* and 1 μM FCCP. Thick line, O_2 concentration (nmol ml^{-1}); thin line, oxygen flux, i.e. negative time derivate of the O_2 concentration (pmol s^{-1} ml^{-1}). *x* axis in hours:minutes:seconds.

carefully removed, washed and stored in 200 μl of solution B for further citrate synthase (CS) activity assay (see below). Respiration rates were expressed in pmol O_2 s^{-1} (mg dry weight)$^{-1}$ or pmol O_2/CS activity.

Citrate synthase activity

After mitochondrial membrane disruption by three consecutive freeze–thaw cycles, CS activity in each fibre bundle was measured spectrophotometrically at 412 nm as previously described (Robinson *et al.* 1987). The reaction was followed for 3 min before and after addition of oxaloacetate. The activity of CS was not influenced by the substrates and inhibitors added during the respirometry experiments, as tested in a preliminary experiment (data not shown). After this measurement, fibre bundles were carefully removed, rinsed with distilled water, evaporated to dryness (60°C, 24 h) and weighed.

Analysis of MyHC content of fibre bundles

Before loading, 10 μl of the Laemmli fibre extracts were diluted with 40 μl of Laemmli ×1 and boiled for 2 min at 100°C for complete MyHC denaturation. Then, 10 μl of the diluted samples were loaded per electrophoresis gel lane. Gradient SDS-PAGE electrophoresis of MyHC was performed according to the method of Sayd *et al.* (1998) with slight modification of the polyacrylamide and glycerol gradients (6–8% and 20–30%, respectively) in the separating gel. Migration was performed at 5°C for 2 h at 70 V followed by 60 h at 130 V, using the Hoefer SE 600 Electrophoresis Unit System (Hoefer, San Francisco, CA, USA). Gels were subsequently stained using the Silver Stain Plus Kit (Bio-Rad, Richmond, CA, USA). The proportions of the different MyHC isoforms were determined using a Bio-Rad gel scanning system (Gel Doc 2000) coupled with the Quantity One (4.0, Bio-Rad) analysis software. A control sample containing all four isoforms was included in each run to precisely identify the different MyHC. The proportion of each MyHC was used to classify the bundles into different contractile types.

Reagents

All reagents were purchased from Sigma (USA) except ATP and ADP, which were obtained from Roche (Germany), and were of the highest quality available.

Statistical analysis

The classification of fibre bundles according to their MyHC composition was achieved using principal component analysis (PCA) and ascending hierarchical classification (SPAD, CISIA, France). The proportion of each MyHC isoform determined by electrophoresis was used as the variable. Data were then analysed by analysis of variance using the generalized linear model procedure of SAS (SAS Institute Inc., Cary, NC, USA). The model included the main effects of fibre class, animal within fibre classes, and their interaction. The effects of calcium, creatine, AMP and glucose on respiration rate were tested within each fibre class using a model including the main effects of treatment (substrate additions), animal within treatment, and their interaction. The main effects were tested against the animal within treatment residual error. Duncan's multiple range tests were used for mean comparisons when the main effects were significant. Significant levels retained were $^{*}P < 0.05$, $^{**}P < 0.01$, $^{***}P < 0.001$. The values were expressed as means ± S.E.M. The apparent K_m^{ADP} were estimated from linear regressions of the double reciprocal plots of the V_{O_2} *versus* ADP relationships and maximization of R^2; the K_m^{ADP} values were calculated from the interpolated point $x_{(y=0)}$ between straight regression line and x axis, according to the Lineweaver–Burck equation $x_{(y=0)} = -1/K_m$. When the relationships was curvilinear, results were confirmed by using the Enzfitter program for enzyme kinetics (BIOSOFT, Cambridge, UK).

Results

Classification of fibre bundles according to MyHC composition

The rabbit was chosen as a model because it has been reported to have muscles containing homogeneous populations of fibres. However, whereas the 55 fibre bundles from the SmP muscle did contain exclusively type I MyHC, and thus corresponded to pure type I fibre bundles, the other muscles did not exhibit such homogeneity; most of the fibre bundles expressed two or three MyHC isoforms (Fig. 2). A PCA coupled with an ascending hierarchical classification was therefore used in order to objectively classify the fibre bundles in TA, PM and SmA muscles. All fibre bundles from these three muscles were included in the analysis. Three major classes were identified within the 166 type II bundles examined: class 2 contained 53 fibre bundles from the TA muscle that expressed both MyHC IIa and IIx (IIa accounting for 46%) and a trace amount of MyHC I (6%). This class was named type IIax. Class 3 was composed of 55 PM muscle fibre bundles expressing 93% MyHC IIx and a trace amount of IIb (7%). It was thus considered as type IIx. Finally, class 4 comprised 52 fibre bundles from the SmA muscle; all expressed the three fast MyHC isoforms (59% IIb, 26% IIx and 15% IIa). Because IIb represented roughly 60% of total MyHC, they were regarded as type IIb dominant (IIb+) fibre bundles. Some fibre bundles from the TA ($n = 3$) and SmA ($n = 3$) muscles were excluded from these three main classes and

A

class	corresponding fiber type	n	muscle	% of MyHC I	IIa	IIx	IIb
1	I	55	SmP	100 ± 0			
2	IIxa	53	TA	5.9 ± 2.1	45.6 ± 4.0	48.5 ± 4.6	
3	IIx	55	PM			92.9 ± 5.4	7.1± 5.4
4	IIb+	52	SmA		15.4 ± 3.2	25.8 ± 7.2	59.0 ± 8.2

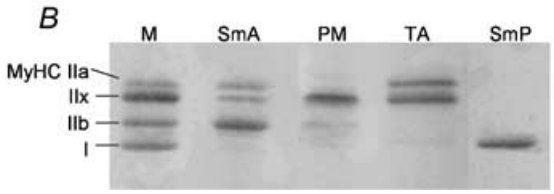

Figure 2. Fibre bundle types
A, fibre bundle classes, or types, delineated by principal component analysis and ascending hierarchical classification based on their MyHC content. *B*, representative SDS-PAGE gels. M, marker; MyHC, myosin heavy chain. Values are means ± S.E.M.

gathered in a fifth class by hierarchical classification. These heterogeneous bundles coexpressed varying levels of three (IIa, IIx, IIb) to four MyHC without any strong dominance of a given isoform. This fifth class was therefore not suitable for analysis of the relationships between fibre types and mitochondrial function.

Respiration rates of *in situ* mitochondria

Because mitochondrial content is quite different between fibre types, respiration rates were normalized to CS activity (a marker of mitochondrial content) to evaluate mitochondrial properties *per se* (Fig. 3). Whereas V_0/CS did not differ significantly between fibre bundle types, V_{max}/CS and ACR were the highest in type I (3.98 ± 0.61 pmol O_2/CS and 5.50 ± 1.09, respectively), intermediate in IIax (2.06 ± 0.38 pmol O_2/CS and 4.21 ± 0.81) and the lowest in IIx (1.74 ± 0.45 pmol O_2/CS and 2.96 ± 0.97) and IIb + (1.73 ± 0.68 pmol O_2/CS and 3.04 ± 0.73) fibre bundles ($P < 0.001$).

Kinetics of respiration regulation by ADP

Figure 4*A* shows Lineweaver–Burk plots of the V_{O_2} *versus* ADP relationships obtained in representative kinetic experiments performed on type I and IIx (upper panel), IIax (middle panel) and IIb+ (lower panel) fibre bundles. Regression analysis revealed two strikingly different K_m^{ADP}

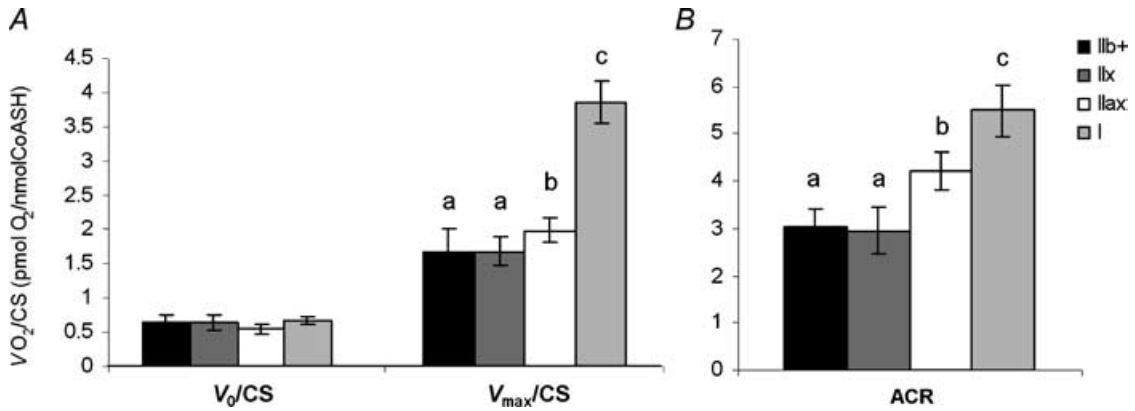

Figure 3. Respiratory parameters of type IIb+, IIx, IIax and I fibre bundles
A, basal (V_0, pyruvate + malate), and maximal (V_{max}, 1 mM ADP) respiration rates measured on saponin-permeabilized fibres and reported relative to citrate synthase (CS) activity. *B*, acceptor control ratio (ACR, V_{max}/V_0). Values are means ± S.E.M. ($n = 8$). Different superscripts denote significantly different values.

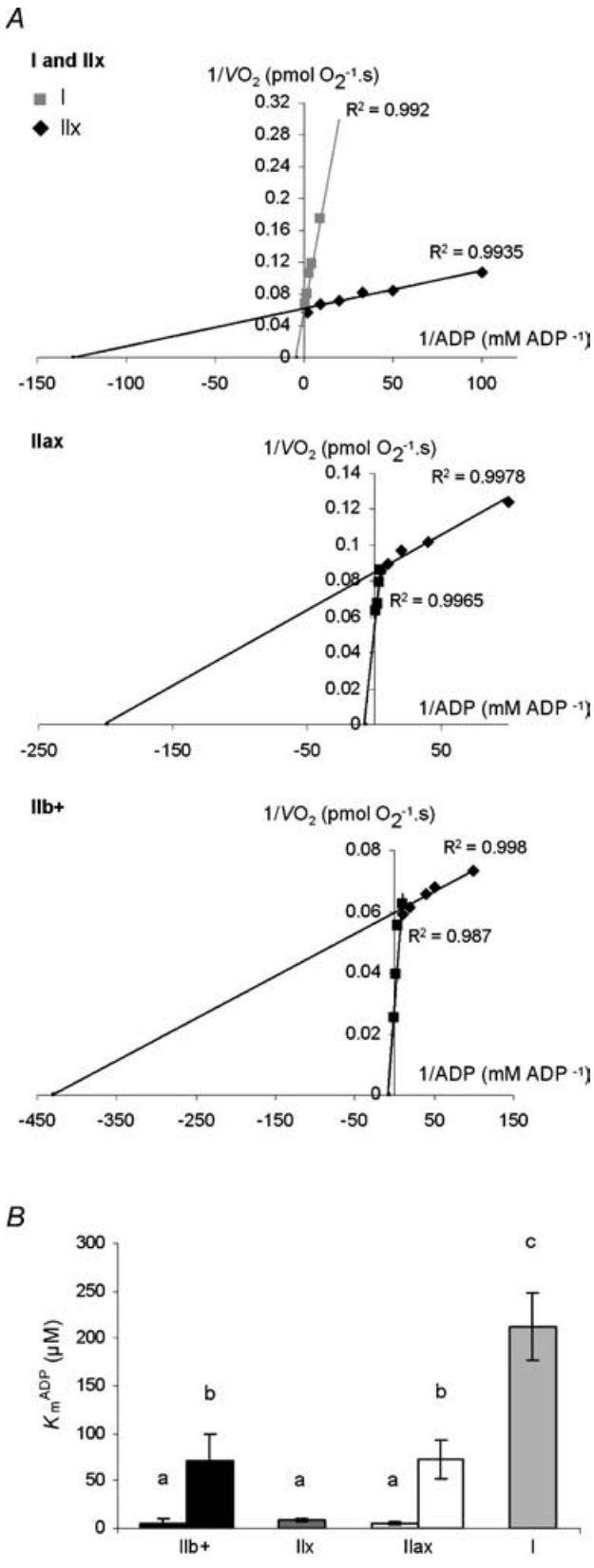

Figure 4. Kinetics of ADP-stimulated respiration in type IIb +, IIx, IIax, and I fibre bundles
A, Lineweaver–Burk linearization of changes in respiration rates as a function of ADP concentration in representative experiments. Upper panel, type I and IIx; middle panel, IIxa; and lower panel, IIb+ fibre bundles. Note that in IIax and IIb+ fibre bundles, two linear segments are delineated by maximization of R^2. *B*, influence of fibre bundle type on mitochondrial apparent K_m for ADP. Values are means ± S.E.M. ($n = 8$). Different superscripts represent significantly different values.

between type I and IIx fibre bundles, with a 25-fold higher value ($P < 0.001$) in type I (212.2 ± 70.7 μM) than IIx (8.0 ± 2.8) fibre bundles (Fig. 4*B*). Clearly different patterns were obtained for mixed fibre bundle types. Indeed, in contrast to the single linear segment observed in type I and IIx fibre bundles, the Lineweaver–Burk plots revealed a systematic deviation from linearity in the experiment performed on IIax and IIb+ bundles. In fact, two linear segments could be identified, with a break point appearing at roughly 0.1 mM ADP. Within each IIax and IIb+ mixed fibre bundle type, a low K_m^{ADP} value (5.0 ± 1.3 and 5.5 ± 4.3, respectively), and an intermediate K_m^{ADP} value (72.0 ± 30.9 and 70.6 ± 28.0) were observed. Intermediate K_m^{ADP} values were similar in IIax and IIb+ fibre bundles (Fig. 4*B*), and the lower K_m^{ADP} did not differ significantly from that obtained in IIx fibre bundles.

Effect of kinase activation on mitochondrial respiration

Figure 5 shows the stimulation of mitochondrial respiration by the addition of substrates of various kinases, i.e. mtCK (Fig. 5*A*), AK2 (Fig. 5*B*) and HK1 (Fig. 5*C*) to each fibre bundle type. To clarify the presentation, the results are reported relative to mitochondrial respiration rates before addition of kinase substrates (i.e. a value of 100 corresponds to the level of respiration before addition of kinase substrates). No creatine effect was observed on submaximal-ADP stimulated respiration in IIb+ and IIx fibre bundles. By contrast, the respiratory rates at 0.1 mM ADP were approximately 20% and 65% higher in IIax and I fibre bundles, respectively ($P < 0.01$). As for creatine, AMP addition did not induce any modification of mitochondrial respiration rates in IIb+ and IIx fibre bundles, but enhanced the submaximal ADP-stimulated respiration ($P < 0.001$) in type IIax (+41.8 ± 14.9%) and type I fibre bundles (+169.0 ± 35.4%). Subsequent inhibition of AK2 by its inhibitor Ap5A restored initial respiration rates. HK1 activation by addition of glucose had no effect on mitochondrial respiration in the various fibre bundle types ($P > 0.05$).

Effect of calcium on regulation of mitochondrial respiration

The presence of 0.4 μM free Ca^{2+} induced an increase in submaximal respiration (0.1 mM ADP) of 17% (tendency $P < 0.1$), 19% ($P < 0.05$), 45% ($P < 0.01$) and 175%

($P < 0.001$) in IIb+, IIx, IIax and I fibre bundles, respectively (Fig. 6*A*). In the initial presence of vanadate, an inhibitor of myosin-ATPase, the stimulatory effect of Ca^{2+} on mitochondrial respiration was prevented in all fibre bundle types.

The ADP sensitivity index was not influenced by addition of calcium in IIb+ and IIx fibre bundles, but increased in IIax (0.78 ± 0.17 *versus* 0.55 ± 0.11, $P < 0.05$) and I (0.67 ± 0.08 *versus* 0.17 ± 0.06, $P < 0.001$) fibre bundles (Fig. 6*B*). The effects of Ca^{2+} were completely prevented in IIax fibre bundles and drastically reduced in type I fibres in the initial presence of vanadate.

Regulation of mitochondrial respiration by creatine and AMP in the presence of calcium was also analysed (Fig. 7). Because no effect of AMP or creatine was observed for type IIx and IIb+ fibre bundles (Fig. 5), only the results for type I and IIax bundles are shown. The stimulation of respiration rates following addition of creatine or AMP was suppressed in the presence of 0.4 μM free Ca^{2+}. However, in the presence of Ca^{2+} and vanadate, the effects of addition of creatine or AMP on mitochondrial respiratory rates were partially restored in type I (+59 and +80% with creatine and AMP, respectively; $P < 0.05$) and IIax (+13 and +20%, $P < 0.05$ and $P < 0.1$, respectively) fibre bundles.

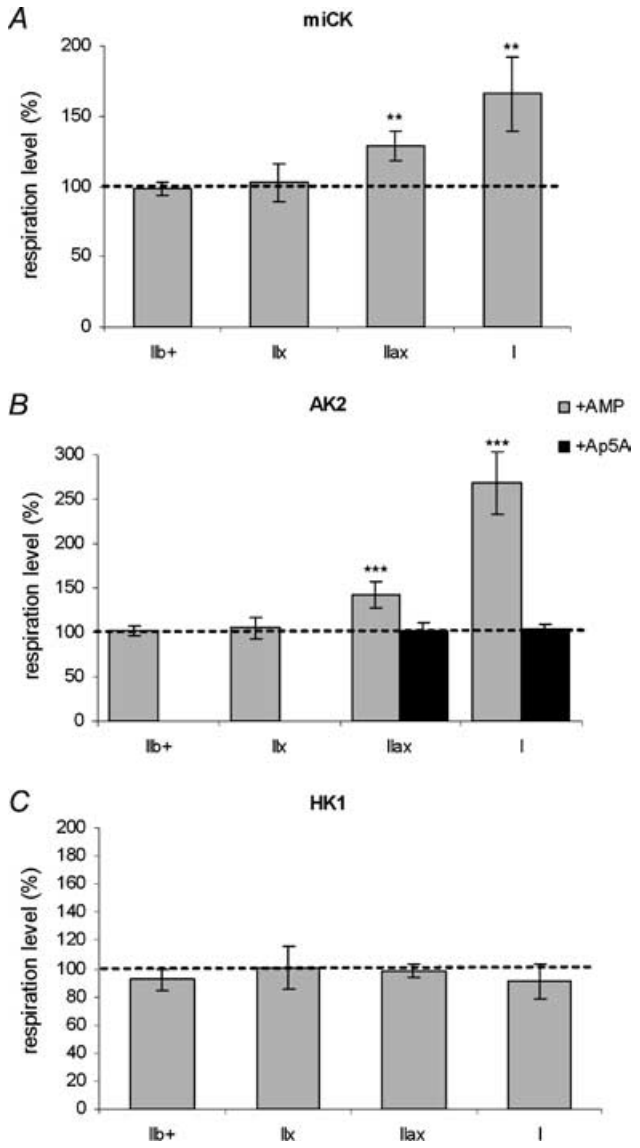

Figure 5. Effect of mitochondrial creatine kinase (mtCK; *A*), adenylate kinase (AK2; *B*) and mitochondria-bound hexokinase (HK1; *C*) activation on submaximal ADP-stimulated respiration in type IIb+, IIx, IIax and I fibre bundles

The effects of stimulation of mtCK (by 20 mM creatine), AK2 (by 1 mM AMP) and HK1 (by 10 mM glucose) are reported relative to mitochondrial respiration rates before substrate addition (a value of 100 corresponds to respiration rates before kinase stimulation). Values are means ± S.E.M. ($n = 6$). Kinase stimulation effects: ***$P < 0.001$; **$P < 0.01$.

Discussion

This study was undertaken to assess the regulation of mitochondrial respiration by ADP, mitochondrial kinases and calcium *in situ* according to muscle fibre type.

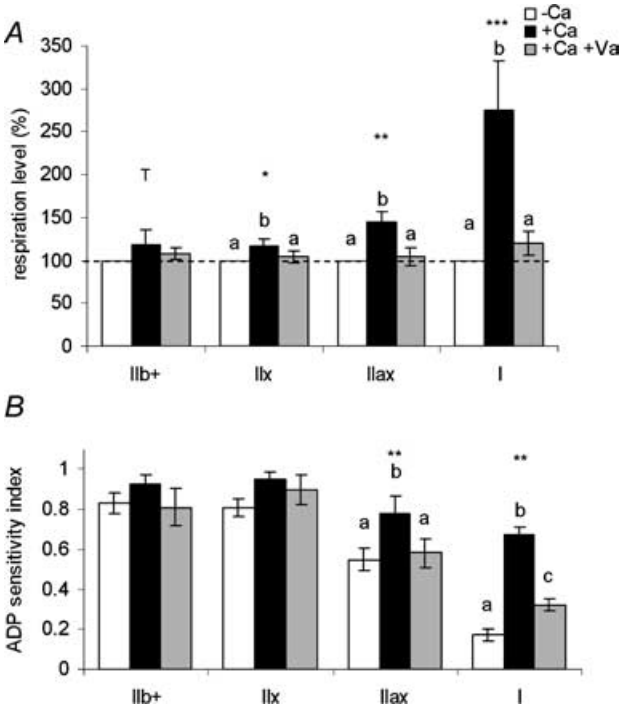

Figure 6. Effect of 0.4 μM free Ca^{2+} in the absence or presence of 0.6 mM vanadate, on submaximal ADP-stimulated respiration (*A*) and ADP sensitivity (*B*) in type IIb+, IIx, IIax and I fibre bundles

A, respiration rates are expressed as a percentage, level 100 corresponding to respiration rates before addition of Ca^{2+}. *B*, the ADP sensitivity index was defined as $V_{(ADP\ 0.1\ mM)}/V_{(ADP\ 1\ mM)}$. +Ca, calcium addition; +Ca + Va, calcium addition in the presence of vanadate. Values are means ± S.E.M. ($n = 6$ for +Ca and 5 for +Ca + Va). Calcium effect: ***$P < 0.001$; **$P < 0.01$; *$P < 0.05$ and *T* (tendency), $P < 0.1$. Different superscripts denote significantly different values within one fibre bundle type.

The four selected rabbit muscles allowed us to obtain four fibre bundle types, i.e. I, IIax, IIx and IIb+. Even though fibre bundle types did not reach our expectations in terms of fibre type homogeneity, the comparison between type IIax and IIx fibre bundles enabled us to get information about specific properties of IIa fibres. Our results indicate that both fibre type and Ca^{2+}-activated myosin-ATPases influence the regulation of mitochondrial function. By contrast with IIx fibres, type I and IIa fibres displayed a specific regulation of mitochondrial respiration characterized by a reduced mitochondrial affinity for ADP and a functional coupling between both mtCK and AK2 and oxidative phosphorylation. Mitochondrial function did not seem to differ between IIx and IIb fibres, but the presence of some IIa fibres along with the IIx fibres in the IIb+ bundles make the specific properties of IIb fibres quite difficult to determine. Our results also demonstrate that the Ca^{2+}-induced activation of myosin-ATPases influences mitochondrial ADP sensitivity and the coupling of mitochondrial kinases with mitochondrial respiration.

Mitochondrial respiration differs between fibre types

In the present study, the maximal oxidative capacity of mitochondria and the coupling between oxidation and phosphorylation (ACR) increased with fibre energy demand. The highest values were observed in type I oxidative fibres followed by IIax bundles, which is likely to be due to the presence of oxido-glycolytic IIa fibres. This is consistent with the higher maximal oxidative capacity and activities of several electron transport chain enzymes found in isolated mitochondria from rabbit type I than IIx/IIb muscles (Jackman & Willis, 1996), and supports the argument for intrinsic differences in mitochondrial function between fibre types.

Regulation of mitochondrial respiration by ADP is fibre type dependent

In accordance with previous studies showing a strikingly lower apparent affinity of mitochondrial respiration for ADP in slow- than fast-twitch muscle (Veksler *et al.* 1995; Kuznetsov *et al.* 1996; Kay *et al.* 1997; Burelle & Hochachka, 2002; Zoll *et al.* 2002), we found an approximately 25 times lower sensitivity of mitochondria to external ADP in type I (K_m^{ADP} 212 μM) than in type IIx fibres (K_m^{ADP} 8 μM). More interestingly, two K_m^{ADP} values were detected within each mixed fibre-type bundle (Fig. 4), i.e. IIax and IIb+, denoting functionally distinct mitochondrial populations. Burelle & Hochachka (2002) also observed two different mitochondrial K_m^{ADP} within fibre bundles from the rat red gastrocnemius, a muscle of mixed fibre type composition. They attributed such a phenomenon to the presence of two functionally distinct mitochondrial populations within the fibre bundles, corresponding either to (i) the subsarcolemmal and intermyofibrillar mitochondria, or (ii) the heterogeneous fibre-type composition of the muscle. Because only one K_m^{ADP} was observed in our pure type I and IIx fibre bundles, where both subsarcolemmal and intermyofibrillar mitochondria are present, the second hypothesis appears far more likely. Thus, the similarity between the low K_m^{ADP} in IIax (5.5 μM) and IIx fibre bundles strongly suggests that the low K_m^{ADP} value in IIax fibre bundles is related to the presence of IIx fibres, and, consequently, that the high K_m^{ADP} value (72 μM) would correspond to mitochondria of IIa fibres. In IIb+ fibre bundles composed of IIb, IIx and IIa fibres, the high K_m^{ADP} value was similar to that obtained in IIax fibre bundles (70 μM), which is likely to be due to the presence of IIa fibres; the low K_m^{ADP} (5 μM) did not differ from that of pure IIx fibres, suggesting no difference in mitochondrial affinity for ADP between IIx and IIb fibres. One could argue that the high K_m^{ADP} in IIax fibre bundles could be due to the presence of a trace amount of type I fibres. However, in this case, the K_m^{ADP} should be in the 200 μM range, and no high K_m^{ADP} value should be observed in IIb+ fibre bundles devoid of type I fibres. These observations strongly support an intermediate

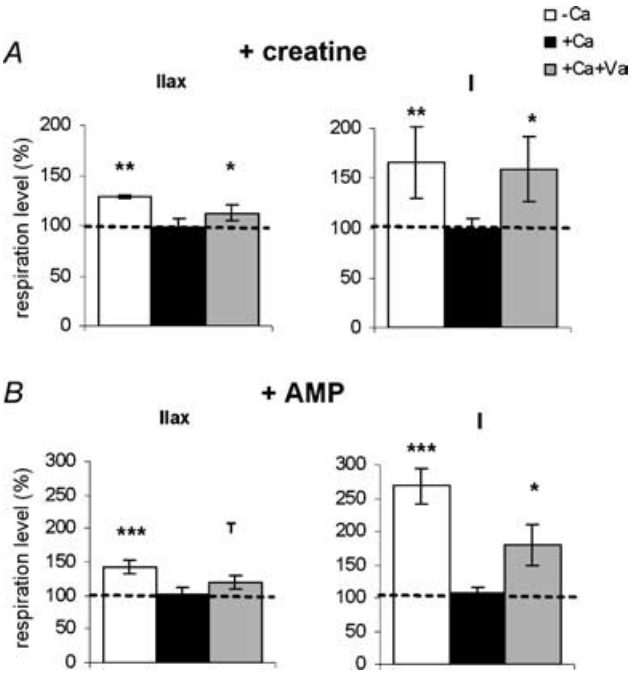

Figure 7. Effect of mitochondrial creatine kinase (mtCK; *A*) and adenylate kinase (AK2; *B*) activation on submaximal ADP-stimulated respiration in type IIax and I fibre bundles, in the absence or presence of 0.4 μM free Ca^{2+} and vanadate
The effects of mtCK (20 mM creatine) and AK2 (1 mM AMP) activation are reported relative to mitochondrial respiration rates before addition of kinase substrates (a value of 100 corresponds to respiration rates before kinase stimulation). Ca, calcium; Va, vanadate. Values are means ± S.E.M. ($n = 6$). Kinase stimulation effects: $^{**}P < 0.01$, $^{*}P < 0.05$ and T, $P < 0.1$.

mitochondrial affinity for ADP in IIa fibres, which means a reduced OMM permeability for ADP. Mitochondrial respiration regulation does not seem to differ between glycolytic types IIb and IIx fibres. Thus, our results confirm the much lower affinity of mitochondria for ADP previously observed in slow- than in fast-twitch muscle fibres, and provide further evidence for a differential regulation of respiration by ADP within fast type II fibres.

Creatine and adenylate kinases are functionally coupled with oxidative phosphorylation

One goal of the present study was to analyse the effect of mtCK activation on mitochondrial respiration according to contractile types of skeletal muscle fibres. The study also included other kinases that may be involved in the regulation of oxidative phosphorylation, i.e. the mitochondrial adenylate kinase, AK2, located in the intermembrane space (Walker & Dow, 1982), and the hexokinase HK1, bound to VDAC at the outside of the OMM (Brdiczka & Wallimann, 1994). Activation of mtCK by creatine induced an increase in respiration rate in type I fibres, and to a lesser extent in type IIax fibre bundles, exclusively (Fig. 5). Since no effect was observed in pure IIx fibre bundles, the creatine effect in IIax bundles could be attributed to mitochondria within IIa fibres. Consistent with previous results in slow-twitch skeletal and cardiac myofibres (Wallimann *et al.* 1992; Saks *et al.* 1994; Kay *et al.* 2000), this increase in submaximal respiration denotes a functional coupling between mtCK and oxidative phosphorylation, leading to an increased local turnover of adenine nucleotides (Wallimann *et al.* 1992; Brdiczka & Wallimann, 1994) in mitochondria of slow type I fibres. Our results also provide further evidence for the existence of such a coupling in mitochondria of fast type IIa fibres; such a coupling does not occur in the fast IIx and probably does not occur in IIb fibres. It is believed that the functional coupling of mtCK to respiration increases the ADP concentration in the vicinity of the ANT and compensates for the barrier to ADP diffusion exerted by OMM (Gellerich *et al.* 1987; Saks *et al.* 1993, 1994; Anflous *et al.* 2001). Thus, the stimulatory effect of creatine on respiration in type I as well as type IIax fibres (but not in type IIx fibres) also supports the reduction of the OMM permeability in type IIa fibres evoked previously. Interestingly, an increase in mitochondrial respiration rate in type I and IIax fibre bundles was also observed following the activation of AK2 by AMP, an effect prevented by the initial presence of the AK inhibitor Ap5A (Fig. 5*B*). These results argue for a functional coupling between AK2 and oxidative phosphorylation in slow/I and fast/IIa fibres. A role for the AK system in energy transfer in skeletal muscle fibres has previously been reported by monitoring [^{18}O]phosphoryl oxygen exchange (Zeleznikar *et al.* 1990, 1995). According to these two studies, the AK was primarily coupled with glycolysis. However, only rat diaphragm, a glycolytic, essentially IIx, muscle, was used and the involvement of the AK system in the transfer of energy-rich phosphoryls from mitochondria to cytosolic ATPase was not investigated in type I and IIa skeletal muscles. In the cardiac muscle, Dzeja *et al.* (1999) demonstrated that both CK and AK systems are involved in high-energy phosphoryl transfer from mitochondria to actomyosin, and catalyse 85 and 10% of the total ATP metabolic rate, respectively. Moreover, the down regulation of CK activity associated with heart failure resulted in an increased contribution of the AK system to cellular energy transfer (Dzeja *et al.* 1999). Thus, the AK and CK systems seem interrelated in cardiac muscle. Our results further show that the AK and CK systems can both catalyse phosphotransfer from mitochondria to myofibrillar and sarcoplasmic ATPases in skeletal type I and IIa fibres. However, the method used here did not allow the determination of the relative importance of each kinase system in exporting high-energy phosphoryls from mitochondria.

In contrast to mtCK and AK2, the stimulation of HK1 by the addition of glucose did not have any effect on mitochondrial respiration, whatever the fibre type, despite the persistence of the association between HK1 and VDAC in permeabilized fibres (Parra *et al.* 1997). Thus, despite the close proximity of HK1 and ANT due to their anchoring to VDAC (Brdiczka & Wallimann, 1994), mitochondria did not exhibit a higher affinity for the local HK1-produced ADP than for the externally added ADP. Preferential use of intramitochondrial generated ATP by membrane-bound HK1 has been demonstrated in liver (Brdiczka & Wallimann, 1994) and skeletal muscle (Parra *et al.* 1997). Our results suggest that the reverse, i.e. direct channelling of HK1-generated ADP to mitochondrial oxidative phosphorylation, does not occur in skeletal fibres. In a reconstituted system including isolated liver mitochondria and dextran, a significant decrease in K_m^{ADP} was observed when mitochondrial respiration was stimulated with ADP locally generated by bound HK; this suggests a functional coupling of bound HK with oxidative phosphorylation. However, liver mitochondria are devoid of mtCK (Miller *et al.* 1997), and it is possible that a specific arrangement of contact sites in the liver (Brdiczka & Wallimann, 1994) allows HK to play the same role in energy transfer as do CK and AK in muscle.

Ca^{2+}-activated myosin ATPase is involved in regulation of mitochondrial respiration in type I and IIax bundles

The presence of a physiological free Ca^{2+} concentration (0.4 μM) (Kummel, 1988; Bers, 2001) increased the submaximal-ADP stimulated respiration rates,

particularly in type I and IIax fibre bundles (Fig. 6). The addition of vanadate, an inhibitor of myosin-ATPase, abolished this calcium effect, whereas vanadate alone did not alter mitochondrial respiration (data not shown). This strongly supports an action of calcium on oxidative phosphorylation mostly *via* the stimulation of actomyosin-ATPase, and not *via* direct activation of mitochondrial dehydrogenases under our experimental conditions (i.e. addition of $CaCl_2$ after stimulation of respiration by ADP). This is consistent with the results of previous studies carried out on human vastus lateralis muscle, using inhibitors of ATPases and the Ca^{2+} transport pathway (Kunz *et al.* 1993) and 'ghost fibres' devoid of myosins (Khuchua *et al.* 1994). Three main mechanisms can be suggested to explain the effect of calcium on mitochondrial respiration. (i) Calcium induces an increase in Ca^{2+}-sensitive myosin-ATPase activity, which, in turn, leads to an increased diffusion of ADP to mitochondria thereby stimulating respiration. (ii) Activation of myosin-ATPase activity by Ca^{2+} is followed by a direct channelling of myosin-ATPase-produced ADP to mitochondria. Indeed, Kummel (1988) first showed in rat myocytes that oxidative phosphorylation and cytoplasmic ATPase activity were functionally coupled. This was illustrated by the apparent preference of oxidative phosphorylation for ADP provided by ATPases (K_m^{ADP} 45 μM) compared to exogenously added ADP (K_m^{ADP} 150 μM). These results were then confirmed by Seppet *et al.* (2001) in permeabilized rat cardiac muscle fibres. Thus, mitochondria in these cells behave as if they were part of functional complexes including adjacent ATPases of myofibrils and of sarcoplasmic reticulum. (iii) Sarcomere contraction due to myosin activation by Ca^{2+} could, through the structural links between mitochondria and myofibrils via cytoskeleton (Appeix *et al.* 2003), induce a deformation of the OMM and opening of the VDAC pores to adenine nucleotides; this in turn results in an increased mitochondrial affinity for ADP (Andrienko *et al.* 2003). Because the effect of Ca^{2+} on oxidative phosphorylation via myosin-ATPase stimulation should have been higher in fast than in slow fibre bundles, due to the increasing actomyosin-ATPase activity in the rank order MyHC I, IIa, IIx and IIb (Bottinelli *et al.* 1994), the first mechanism is not consistent with our results (Fig. 6*A*). Indeed, we showed a higher Ca^{2+}-induced increase in submaximal respiration in type I (+175%) than in type II fibres (+45%, 17% and 19% in IIax, IIx and IIb+ bundles, respectively). In contrast, our results (Fig. 6*B*) show a 250% and 45% Ca^{2+}-induced increase in mitochondrial sensitivity to ADP in type I and IIax fibre bundles, respectively, strictly parallel with the corresponding increases in respiration rates, and almost prevented in the presence of the myosin-ATPase inhibitor. They are consistent with the second and third hypothesis. Indeed, these two mechanisms both result in a decrease in mitochondrial K_m^{ADP} (Kummel, 1988; Seppet *et al.* 2001; Andrienko *et al.* 2003).

In the presence of Ca^{2+}, addition of the respective substrates of mtCK and AK2, creatine and AMP, no longer stimulated submaximal ADP-stimulated respiration (Fig. 7), suggesting that these mitochondrial kinases were no longer functionally coupled with oxidative phosphorylation. In line with our observations, using ^{31}P NMR, Joubert *et al.* (2002) analysed the subcellular phosphocreatine/creatine fluxes linked to the CK reaction in beating cardiac muscle, and concluded that the control strength exerted by the mtCK on the energy transfer may depend on cardiac contractile activity. Even so, our results seem quite surprising, because they suggest that an increase in energy need due to fibre contraction would be coupled with a decreased efficacy of the high-energy phosphoryl transfer system. However, this phenomenon is not illogical if one admits the second hypothesis described above, namely a direct coupling between mitochondria and myosin following Ca^{2+}-induced activation of myosin-ATPase. In this case, different energy transfer pathways would coexist within the oxidative type I and IIa fibres, i.e. CK- and AK-catalysed phosphotransfer, and a direct transfer of adenine nucleotides; the relative importance of each system would depend on the contractile activity of the myofibre. Thus, the Ca^{2+}-induced activation of myosin-ATPase would favour direct channelling of ADP between myosin and mitochondria compared to CK- and AK-catalysed phosphotransfer. Finally, the dramatic Ca^{2+}-induced increase in mitochondrial sensitivity to ADP in type I and IIax fibre bundles, close to that obtained in IIx and IIb+ fibre bundles, could explain the absence of functional coupling between mitochondrial kinases and oxidative phosphorylation in the presence of calcium, since this coupling relies both on structural interactions of kinases with ANT and VDAC (Wallimann *et al.* 1992) and on restricted mitochondrial affinity to cytosolic ADP.

Conclusion

In light of our results, two models of muscle fibre functioning can be proposed. In fibres whose contraction mostly relies on glycolytic metabolism (IIb, IIx), mitochondrial respiration is not specifically controlled and it participates essentially in the recovery of the phosphocreatine level. On the contrary, in addition to a high maximal respiration and oxidation–phosphorylation coupling, mitochondria within fibres whose contraction is fuelled by oxidative metabolism (I and IIa) exhibit a restricted sensitivity to cytosolic ADP; this allows efficient coupling between ATP production and mitochondrial kinases located in the intermembrane space. In these fibres, at least three energy transfer systems could be involved in the matching between ATP demand and

synthesis: the CK- and AK-catalysed phosphotransfer and a direct channelling of adenine nucleotides between myosin-ATPase and mitochondria. During contraction, the direct channelling could progressively overcome the CK and AK systems. However, although our data indicate a close link that is of a functional and/or structural nature between myosin-ATPase and mitochondria, understanding the exact mechanism involved in the regulation of mitochondrial respiration by Ca^{2+}-induced activation of myosin-ATPase requires further investigations.

References

Andrienko T, Kuznetsov AV, Kaambre T, Usson Y, Orosco A, Appaix F *et al.* (2003). Metabolic consequences of functional complexes of mitochondria, myofibrils and sarcoplasmic reticulum in muscle cells. *J Exp Biol* **206**, 2059–2072.

Anflous K, Armstrong DD & Craigen WJ (2001). Altered mitochondrial sensitivity for ADP and maintenance of creatine-stimulated respiration in oxidative striated muscles from VDAC1-deficient mice. *J Biol Chem* **276**, 1954–1960.

Appeix F, Kuznetsov AV, Usson Y, Kay L, Andrienko T, Olivares J *et al.* (2003). Possible role of cytoskeleton in intracellular arrangement and regulation of mitochondria. *Exp Physiol* **88**, 175–190.

Berchtold MW, Brinkmeier H & Munter M (2000). Calcium ion in skeletal muscle: its crucial role for muscle function, plasticity and disease. *Physiol Rev* **80**, 1215–1565.

Bers D (2001). *Excitation-Contraction Coupling and Cardiac Contraction*. Kluwer, Dordrecht.

Bottinelli R, Canepari M & Reggiani C (1994). Myofibrillar ATPase activity during isometric contraction and isomyosin composition from skinned rat skeletal muscle. *J Physiol* **481**, 663–675.

Brdiczka D & Wallimann T (1994). The importance of the outer mitochondrial compartment in regulation of energy metabolism. *Mol Cell Biochem* **133/134**, 69–83.

Bruton JD, Dahlsted AJ, Abbate F & Westerblad H (2003). Mitochondrial function in intact skeletal muscle fibres of creatine kinase deficient mice. *J Physiol* **552**, 393–402.

Burelle Y & Hochachka PW (2002). Endurance training induced muscle-specific changes in mitochondrial function in skinned muscle fibers. *J Appl Physiol* **92**, 2429–2438.

Clark JF, Kuznetsov AV & Radda GK (1997). ADP-regenerated enzyme systems in mitochondria of guinea pig myometrium and heart. *Am J Physiol* **272**, C399–C404.

Dzeja PP, Kalvenas A, Toleikis A & Praskevicious A (1983). Functional coupling of creatine phosphokinase and adenylate kinase with adenine nucleotide translocase and its role in regulation of heart mitochondrial preparation. *Biokhimiia* **48**, 1471–1478.

Dzeja P, Kalvenas A, Toleikis A & Praskevicius A (1985). The effect of adenylate kinase activity on the rate and efficiency of energy transport from mitochondria to hexokinase. *Biochem Int* **10**, 259–265.

Dzeja PP, Vitkevicius KT, Redfield MM, Burnett JC & Terzic A (1999). Adenylate kinase-catalyzed phosphotransfer in the myocardium. Increased contribution in heart failure. *Circ Res* **84**, 1137–1143.

Dzeja PP, Zeleznikar RJ & Goldberg ND (1996). Suppression of creatine kinase-catalyzed phosphotransfer results in increased phosphoryl transfer by adenylate kinase in intact skeletal muscle. *J Biol Chem* **271**, 12847–12851.

Gellerich FN, Schlame M, Bohnensack R & Kunz W (1987). Dynamic compartmentation of adenine nucleotides in the mitochondrial intermembrane space of rat-heart mitochondria. *Biochim Biophys Acta* **890**, 117–126.

Gnaiger E (2001). Bioenergetics at low oxygen: dependence of respiration and phosphorylation on oxygen and adenosine diphosphate supply. *Respir Physiol* **128**, 277–297.

Gondret F, Lefaucheur L, D'Albis A & Bonneau M (1996). Myosin isoform transitions in four rabbit muscles during postnatal growth. *J Muscle Res Cell Motil* **17**, 657–667.

Hamada M, Takenada H, Fukumoto K, Fukamachi T, Yamaguchi T, Sumida M *et al.* (1987). Structure and function of adenylate kinase isoenzymes in normal humans and muscular dystrophy patients. In *Isoenzymes: Current Topics in Biological and Medical Research*, ed. Marckert CL, Scandolios JG, pp. 81–99. Liss, New York.

Jackman MR & Willis WT (1996). Characteristics of mitochondria isolated from type I and type IIb skeletal muscle. *Am J Physiol* **270**, C673–C678.

Jacobus WE, Moreadith RW & Vandegaer KM (1982). Mitochondrial respiratory control: Evidence against the regulation of respiration by extramitochondrial phosphorylation potentials or by [ATP]/[ADP] ratios. *J Biol Chem* **257**, 2397–2402.

Joubert F, Mazet JL, Mateo P & Hoerter JA (2002). ^{31}P NMR detection of subcellular creatine fluxes in the perfused rat heart. Contractility modifies energy transfer pathways. *J Biol Chem* **277**, 18469–18476.

Kay L, Li Z, Mericskay M, Olivares J, Tranqui L, Fontaine E *et al.* (1997). Study of regulation of mitochondrial regulation in vivo. An analysis of influence of ADP diffusion and possible role of cytoskeleton. *Biochim Biophys Acta* **1322**, 41–59.

Kay L, Nicolay K, Wierenga B, Saks V & Wallimann T (2000). Direct evidence for the control of mitochondrial respiration by mitochondrial creatine kinase in oxidative muscle cells in situ. *J Biol Chem* **275**, 6937–6944.

Khuchua Z, Belikova Y, Kuznetsov AV, Gellerich FN, Schild L, Neumann HW *et al.* (1994). Caffeine and Ca^{2+} stimulate mitochondrial oxidative phosphorylation in saponin-skinned human skeletal muscle fibers due to activation of actomyosin ATPase. *Biochim Biophys Acta* **1188**, 373–379.

Kummel L (1988). Ca,Mg-ATPase activity of permeabilised rat heart cells and its functional coupling to oxidative phosphorylation of the cells. *Cardiovasc Res* **22**, 359–367.

Kunz WS, Kuznetsov AV & Gellerich FN (1993). Mitochondrial oxidative phosphorylation in saponin-skinned human muscle fibers is stimulated by caffeine. *FEBS Lett* **323**, 188–190.

Kuznetsov AV, Tiivel T, Sikk P, Kaambre T, Kay L, Daneshrad Z *et al.* (1996). Striking differences between the kinetics of regulation of respiration by ADP in slow-twitch and fast-twitch muscles in vivo. *Eur J Biochem* **241**, 909–915.

Martonosi N & Pikula S (2003). The network of calcium regulation in muscle. *Acta Biochim Pol* **50**, 1–30.

McKoy G, Léger ME, Bacou F & Goldspink G (1998). Differential expression of myosin heavy chain mRNA and protein isoforms in four functionally diverse rabbit skeletal muscles during pre- and postnatal development. *Dev Dyn* **211**, 193–203.

Miller K, Sharer K, Suhan J & Koretsky AP (1997). Expression of functional mitochondrial creatine kinase in liver of transgenic mice. *Am J Physiol* **272**, C1193–C1202.

Parra J, Brdiczka D, Cusso R & Pette D (1997). Enhanced catalytic activity of hexokinase by work-induced mitochondrial binding in fast-twitch muscle rat. *FEBS Lett* **403**, 279–282.

Pellegrino MA, Canepari M, Rossi R, D'Antona G, Reggiani C & Bottinelli R (2003). Orthologous myosin isoforms and scaling of shortening velocity with body size in mouse, rat, rabbit and human muscles. *J Physiol* **546**, 677–689.

Robinson JB, Brent LG, Sumegi B & Srere PA (1987). In *Mitochondria: a Practical Approach*, ed. Darley-Usmar VM, Rickwood D, Wilson MI, pp. 153–170. IRL Press, Oxford.

Saks VA, Khuchua ZA, Vasilyeva EV, Belikova O & Yu & Kuznetsov AV (1994). Metabolic compartmentation and substrate channelling in muscle cells. Role of coupled creatine kinases in in vivo regulation of cellular respiration – a synthesis. *Mol Cell Biochem* **133/134**, 155–192.

Saks VA, Vassylyeva EV, Belikova YuO, Kuznetsov AV, Lyapina SA, Petrova L *et al.* (1993). Retarded diffusion of ADP in cardiomyocytes: possible role of outer mitochondrial membrane and creatine kinase in cellular regulation of oxidative phosphorylation. *Biochim Biophys Acta* **1144**, 134–148.

Saks VA, Veksler VI, Kuznetsov AV, Kay L, Sikk P, Tiivel T *et al.* (1998). Permeabilized cell and skinned fiber techniques in studies of mitochondrial function in vivo. *Mol Cell Biochem* **184**, 81–100.

Saupe KW, Spinder M, Tian R & Ingwall JS (1998). Impaired cardiac energetics in mice lacking muscle-specific creatine kinase. *Circ Res* **82**, 898–907.

Savabi F, Geiger PJ & Bessman SP (1986). Myokinase and contractile function of glycerinated muscle fibers. *Biochem Med Metab Biol* **35**, 227–238.

Sayd T, Mera T, Martin V & Laville E (1998). Spatial distribution of myosin heavy chain isoforms and lactate dehydrogenase M4 in the limb musculature of two crossbred lambs. *Comp Biochem Physiol B* **120**, 153–163.

Seppet EK, Kaambre T, Sikk P, Tiivel T, Vija H, Tonkonogi M *et al.* (2001). Functional complexes of mitochondria with Ca,MgATPases of myofibrils and sarcoplasmic reticulum in muscle cells. *Biochim Biophys Acta* **1504**, 379–395.

Steeghs K, Benders A, Oerlemans F, de Haan A, Heerschap A, Ruitenberg W *et al.* (1997). Altered Ca^{2+} responses in muscle with combined mitochondrial and cytosolic deficiencies. *Cell* **89**, 93–103.

Tonkonogi M, Harris B & Sahlin K (1998). Mitochondrial oxidative function in human saponin-skinned muscle fibres: effects of prolonged exercise. *J Physiol* **510**, 279–286.

Valentine WN, Paglia DE, Nakatani M & Brockway RA (1989). Inhibition of adenylate kinase by P1,P5-di (adenosine 5′) pentaphosphate in assays of erythrocyte enzyme activities requiring adenine nucleotides. *Am J Hematol* **32**, 143–145.

Veksler VI, Kuznetsov AV, Anflous K, Mateo P, Van Deursen J, Wierenga B *et al.* (1995). Muscle creatine kinase-deficient mice. II. Cardiac and skeletal muscles exhibit tissue-specific adaptation of the mitochondrial function. *J Biol Chem* **270**, 19921–19929.

Walker EJ & Dow JW (1982). Location and properties of two isoenzymes of cardiac adenylate kinase. *Biochem J* **203**, 361–369.

Wallimann T, Wyss M, Brdiczka D, Nicolay K & Eppenberger HM (1992). Intracellular compartmentation, structure and function of creatine kinase isoenzymes in tissues with high and fluctuating energy demands: the 'phosphocreatine circuit' for cellular energy homeostasis. *Biochem J* **281**, 21–40.

Watanabe K, Itakura T & Kubo S (1979). Distribution of adenylate kinase isoenzymes in porcine tissues and their subcellular localization. *J Biochem* **85**, 799–805.

Zeleznikar RJ, Dzeja PP & Goldberg ND (1995). Adenylate kinase-catalyzed phosphoryl transfer couples ATP utilization with its generation by glycolysis in intact muscle. *J Biol Chem* **270**, 7311–7319.

Zeleznikar RJ, Heyman RA, Graeff RM, Walseth TF, Dawis SM, Butz EA *et al.* (1990). Evidence for compartmentalized adenylate kinase catalysis serving a high energy phosphoryl transfer function in rat skeletal muscle. *J Biol Chem* **265**, 300–311.

Zoll J, Koulmann N, Lahougne B, Ventura-Clapier R & Bigard AX (2002). Quantitative and qualitative adaptation of skeletal muscle mitochondria to increased physical activity. *J Cell Physiol* **194**, 186–193.

Acknowledgements

This work was supported by grants from the Institut National de la Recherche Agronomique and the Institut National de la Santé et de la Recherche Médicale (ATC Nutrition INRA/INSERM). N.G. held a fellowship from the Région Bretagne and INRA.

Supplemental material

The online version of this paper can be accessed at:
DOI: 10.1113/jphysiol.2005.083030
http://jp.physoc.org/cgi/content/full/jphysiol.2005.083030/DC1
and contains supplemental material consisting of a figure entitled: Principal component analysis of the distribution of fibre bundles according to the percentage of MyHC I, IIa, IIx and IIb expressed in the bundles.
This material can also be found at:
http://www.blackwellpublishing.com/products/journals/suppmat/tjp/tjp818/tjp818sm.htm